A WIGNER-VILLE, TIME-FREQUENCY APPROACH TO TNT DETECTION IN NUCLEAR QUADRUPOLE RESONANCE EXPERIMENTS.

Sven Aerts[1], *Diederik Aerts*[2], *Franklin E. Schroeck*[3], *and Jürgen Sachs*[4]

[1,2] CLEA, Free University of Brussels
Krijgskundestraat 33, 1160 Brussels, Belgium
email: saerts@vub.ac.be, diraerts@vub.ac.be

[3] Departement of Mathematics, University of Denver
John Greene Hall, 2360 S. Gaylord St., USA
email: fschroec@du.edu

[4] Institut fur Informationstechnik, Technical University of Ilmenau
PF 100565, D-96684, Germany
email: sac@e-technik.tu-ilmenau.de

ABSTRACT

To minimize the risks involved in humanitarian demining requires a sensitivity setting close to unity, resulting in a very high false alarm rate. Nuclear quadrupole resonance detection, based on the spin echoes from nuclear spin relaxation, is a promising example of a highly specific detector that directly addresses the properties of the explosive rather than the mine casing. However, the data aquisition time necessary to obtain a sufficiently high sensitivity is long due to the extremely poor signal-to-noise-ratio of the spin echoes. Besides improvements in the hardware, it is important to pursue better signal analytic techniques. We present a time-frequency approach based on the Wigner-Ville quasi-distribution for the analysis of nuclear quadrupole resonance data. We calculate ROC curves for real data obtained under laboratory conditions and show the technique presents a substantial improvement over popular demodulation techniques, especially for signals with poor signal-to-noise ratio.

1. INTRODUCTION: LANDMINES AND NUCLEAR QUADRUPOLE RESONANCE

In spite of all technological developments, the metal detector remains the detector of choice for most field workers working in the demining area. Even plastic mines can be found by the metal detector, as the detonator always contains a small amount of metal. However, to reliably detect even plastic landmines, sub-gram quantities of metal must be registered. Because a former battle field is often filled with metal debris, this results in an unacceptably high false alarm rate. On average 500 to 1000 objects are wrongly classified as potential mines for each real mine encountered. A promising solution consists of using nuclear quadrupole resonance (NQR) techniques. A necessary condition for the use of NQR, is the presence of a substance with a nuclear quadrupole moment. All known explosives contain the naturally stable nitrogen isotope ^{14}N, (with a natural abundance of 99.64 %) with nuclear spin 1, and with nuclear transitions in the frequency range between 0 and 6 MHz. The transition frequencies depend mostly on the electric field gradient tensor, which is in good approximation determined by the charge distribution of the electrons that bind the nitrogen to the rest of the explosive [1]. NQR signals are therefore highly specific with respect to the chemical structure of the sample, which in turn yields a very reliable classification (very low false alarm rate). Because of its high potential value in remote explosive detection, there is renewed interest in NQR methods for landmine and unexploded ordnance (UXO) detection, as well as for securing crowded high risk areas such as airports by non-intrusive means. The main challenge for NQR techniques, is the extremely poor signal-to-noise-ratio (SNR). To improve the SNR, many repetitions of the experiment are necessary. The most popular method is to set up an appropriate sequence of RF pulses, and register the returned echo after each such pulse. The rate at which repetition is physically informative, is bound from below in a fundamental way by the physical parameters of the nuclear relaxation process, which is a result of two different mechanisms, called the spin-spin relaxation and the spin-lattice relaxation. The relaxation time that characterizes the spin-lattice relaxation, denoted T_1, determines the time necessary for the system to regain its original thermal equilibrium state, and gives a bound on how quickly a pulse sequence can be initiated after another. The spin-spin relaxation time, denoted T_2, is indicative of the decoherence as a result of spin-spin interactions and determines the length of the spin echo sequence. Spin-spin relaxation times are generally (much) shorter than spin-lattice relaxation times. In practice, we can apply a pulse sequence of length T_2, and repeat this pulse sequence every T_1. For most explosives, the relaxation times are short enough so that NQR detection becomes feasible. Unfortunately, this is not feasible for $\alpha-$trinitrotoluene, better known as TNT, the active compound of approximately 60% of the landmines, because TNT has relaxation times that lead to prohibitively long detection times within the operational limits of landmine detection [2]. Because one cannot shorten the relaxation parameters of TNT, much effort has gone into cleverly designing the emitted RF pulse and increasing the sensitivity of the receiver. Besides these efforts, it is worthwhile to pursue better signal analytic detection techniques.

2. THE NUCLEAR QUADRUPOLE RESONANCE SIGNAL

The cause of the NQR signal is the change in the magnetization along the direction of the solenoid. In the case of ^{14}N, we are dealing with a spin-1 system so that the relevant quantum mechanical subspace is spanned by just three orthogonal vectors. Different orientations of the principle axis of the electric field tensor in the crystalline structure, as well as the high temperature, lead to classical statistical mixtures of such spin 1 systems. To accommodate for this fact, theoretical descriptions of NQR ([1], [3], and [5]), describe the state of the system as a classical statistical mixture of pure quantum states using a density operator ρ belonging to the class of linear, positive operators that sum to one when they act upon a complete set of eigenvectors. The dynamics of the density operator ρ is gov-

erned by the unitary evolution that solves the Schrödinger equation

$$\frac{d\rho(t)}{dt} = -\frac{i}{\hbar}[\mathscr{H}, \rho(0)].$$

Here $\hbar$ is the Plank constant divided by 2π, $\mathscr{H}$ is the Hamiltonian of the NQR subsystem and $\rho(0)$ the initial density operator. Data analysis for NQR experiments starts from the quadrature components $V(t)$, which are a result of the change in the magnetization M. The expectation of the magnetization in the direction of the axis of symmetry of the solenoid (say, the z-axis), is obtained by tracing over the product of the state ρ_{sys} (the mixture of quadrupole active spin-1 states) with the magnetization operator $\hat{M}_z$ along that spatial axis:

$$\langle \hat{M}_z \rangle = Tr(\hat{M}_z \rho_{sys}).$$

With N the number of turns in a solenoid of area A, μ the magnetic permeability and Q the quality factor of the coil, we have

$$V(t) = QN\frac{d(\mu M_z A)}{dt}.$$

As the two quadrature components are always 90 degrees out of phase, they form a single complex quantity which can conveniently be expressed in a single real function, known as the Wigner-Ville (time-frequency) quasi-distribution. We will also refer to the Wigner-Ville quasi-distribution as the Wigner-Ville function, or simply the Wigner function.

3. WIGNER FUNCTIONS

We will briefly derive a few properties of Wigner functions in a transparent way that will aid us in the subsequent analysis. Let $x(t), y(t) \in \mathscr{L}_2$ be two complex valued, square integrable functions. These functions could represent signals in signal analysis or states in quantum mechanics. Let $A : \mathscr{L}_2 \times \mathscr{L}_2 \times \mathbb{R} \to \mathscr{L}_1$ be the bilinear quantity

$$A_\tau(x(t), y(t)) = x(t+\tau/2)y^*(t-\tau/2). \tag{1}$$

The function A can be regarded as a parametrized version of the sesquilinear product, which is recovered for $\tau = 0$. The Wigner-Ville joint time-frequency distribution of a temporal function $x(t)$, is defined as:

$$W[x](t,\nu) = \int x(t+\tau/2)x^*(t-\tau/2)\exp(-2\pi i\nu\tau)d\tau. \tag{2}$$

If we denote by $F^\tau[.]$ the usual Fourier transform with respect to τ and define

$$W_{x\cdot y} \equiv F^\tau[A_\tau(x,y)].$$

Then we see that the Wigner function is the Fourier transform of this $\tau-$parametrized product:

$$W_{x\cdot x}(t,\nu) = F^\tau[A_\tau(x,x)](t,\nu) = W[x](t,\nu).$$

For any complex constant a, the Wigner transform satisfies the property

$$W_{ax\cdot ax} = aa^* W_{x\cdot x}$$

It is well-known that, because the Wigner transform is bilinear in its arguments, it fails to be additive in general:

$$W_{(x+y)\cdot(x+y)} \neq W_{x\cdot x} + W_{y\cdot y}$$

One can establish the Wigner transform for the sum of two signals, by noting that, according to (1):

$$\begin{aligned} & A_\tau(x+y,x+y) \\ = \;& A_\tau(x,x) + A_\tau(y,y) + A_\tau(y,x) + A_\tau(x,y) \end{aligned}$$

So that the following rather nice distributive law holds:

$$\begin{aligned} W_{(x+y)\cdot(x+y)} &= F^\tau[A_\tau(x+y,x+y)] \\ &= W_{x\cdot x} + W_{y\cdot y} + W_{x\cdot y} + W_{y\cdot x} \end{aligned}$$

Without additional knowledge, one cannot simplify $W_{x\cdot x} + W_{y\cdot y}$ any further., but the last two terms, $W_{x\cdot y} + W_{y\cdot x}$, can be simplified using (1) to obtain:

$$W_{x\cdot y} + W_{y\cdot x} = F^\tau[A_\tau(y,x)] + F^\tau[A_\tau(x,y)]$$

One can see from the definition of A, that it is invariant if we interchange the order of the signals, invert the sign of τ and take the complex conjugate:

$$A_\tau(y(t),x(t)) = A^*_{-\tau}(x(t),y(t))$$

But for the Fourier transform of A we can say more because of the reflection properties of the Fourier transform. If we denote $F^t[f(t)] = S(\omega)$, then the reflection properties are

$$\begin{aligned} F^t[f(-t)] &= S(-\omega) \\ F^t[f^*(t)] &= S^*(-\omega) \end{aligned}$$

These last two equations can be combined to yield $F^t[f^*(-t)] = S^*(\omega) = F^{t*}[f(t)]$. Then

$$F^\tau[A^*_{-\tau}(x,y)] = F^{\tau*}[A_\tau(x,y)]$$

and it then follows easily that

$$W_{x\cdot y} + W_{y\cdot x} = 2\,\mathrm{Re}(F^\tau[A_\tau(x,y)])$$

and

$$W_{(x+y)\cdot(x+y)} = W_{x\cdot x} + W_{y\cdot y} + 2\,\mathrm{Re}(W_{x\cdot y}) \tag{3}$$

As is well-known, the Wigner function is not necessarily positive for all points in (t,ν) space [4], but it is always real. We see that the non-linear structure of the addition gives rise to extra terms for the resulting Wigner function. We note in passing that the Wigner-Ville time-frequency (quasi) distribution, although formally identical to its quantum mechanical counterpart, has a radically different meaning. In fact, the quantum version is not directly measurable by a single measurement, nor by a repetition of that same experiment. One way to determine the quantum Wigner function is to obtain precise expectation values for a set of observables that form a so-called *quorum*. Such a quorum has the property of being *informationally complete* in Prugovecki's sense, in that it allows for a unique determination of the quantum state of the system. Such a set always contains at least two incompatible observables, whereas we are here referring to the repeated measurement of a single observable. For details, we refer to [7]. In this paper the Wigner function is used in its signal-analytic sense, where it is used as a discrete bilinear transform of the time series that allows for a joint representation of time and frequency information of the signal. In the signal-analysis research community much work has been devoted to generate Wigner-Ville like functions without such "spurious", "ghost" or "interference" peaks by means of appropriately chosen integral kernels in the definition of the Wigner-Ville function, or by convolution. This has given rise to a multitude of different distributions (Pseudo Wigner-Ville, s-Wigner-Ville, Choï-Williams, Born-Jordan,...) depending on which properties one wants the resulting distribution to have [4]. There are however deep theoretical reasons for preferring the Wigner-Ville distribution [7]. While the interference terms may complicate the interpretation of the function, they also ensure the unitary character of the function regarded as a transform. Unitarity, in turn, is a sufficient condition for invertibility of the transform. This means, in effect, that no information was lost in transforming the signal. Rather than making an attempt to minimize the interference terms, we will show they can be exploited to our advantage for detection purposes.

4. A DISTANCE MEASURE ON THE SPACE OF WIGNER FUNCTIONS

We often encounter instances in the literature that employ heuristic "distance measures" for Wigner-Ville functions, such as the Euclidean distance between the first few singular values of the singular value decomposition of the Wigner-Ville function. Of course the Euclidean distance is a true metric in Euclidean space, but such a measure, useful as it may be, fails to be a true metric for the Wigner-Ville functions from which the singular values were calculated. However, it is possible to derive a true distance measure between two Wigner functions. It is well-known that the function

$$d_R(\tilde{x},\tilde{y}) = \arccos|\langle x,y\rangle|. \tag{4}$$

is the natural Riemannian metric between two rays $\tilde{x}$ and $\tilde{y}$ in a Hilbert space $\mathscr{H}$ of which x and y are two unit vector representatives. A Riemannian metric is a positive quadratic form on a Riemann space (i.e., a space that is locally isomorphic to a Euclidean space). Moreover, it is clearly invariant under unitary transformations because the defining feature of a unitary transformation U is:

$$\langle x,y\rangle = \langle Ux,Uy\rangle$$

Vice versa, we have that every invariant metric that provides for a distance between two elements of $\mathscr{H}$, must be a function of $d_R(x,y)$. Suppose that $D(x,y)$ is another invariant metric and that u, $v \in \mathscr{H}$ are arbitrary but such that $d_R(x,y) = d_R(u,v)$. Because any ray can be obtained from any other ray by a unitary transformation, there exist a unitary transformation U_1 such that $x = U_1(u)$. Because U_1 did not change the angle, there exists a second unitary transformation that leaves the ray u invariant and transforms v into $y : y = U_2(v)$. If we set $U = U_1U_2$, then $D(u,v) = D(U(u),U(v)) = D(x,y)$. If $D(x,y) = \alpha(d_R(x,y))$, then we see that $D(u,v) = \alpha(d_R(x,y))$. There is a beautiful and simple relation between the inner product of two vectors and the overlap of two corresponding Wigner functions, called Moyal's formula [6]:

$$\int\int W_{x\cdot x}W_{y\cdot y}dtd\nu = |\int x(t)y^*(t)dt|^2 = |\langle x,y\rangle|^2. \tag{5}$$

Moyal's relation allows to establish a distance measure on the space of Wigner functions. A function $d : X \times X \to \mathbb{R}$ is called a distance measure if it is non-negative and finite, zero only for two identical elements of X, symmetrical in its arguments and satisfies the triangle inequality. Because d_R is a metric, we can quite simply obtain a metric for the Wigner function. Substitution of (5) in (4), we obtain:

$$d(W_{x\cdot x},W_{y\cdot y}) = \arccos\sqrt{\int\int W_{x\cdot x}W_{y\cdot y}dtd\nu}. \tag{6}$$

The former equation is to be understood for Wigner transforms of the unit norm Hilbert space representatives. We note a difference with respect to the metric d_R in L^2, because $d_R(x,y) = 0$ implies $x(t) = e^{i\alpha}y(t)$. Hence, the space which becomes a metric space through d_R, is not the vector space directly, but rather the space whose elements are equivalence classes of vectors of the kind $e^{i\alpha}y(t)$. In other words, it is a metric space with respect to the projective Hilbert space, or the *rays* in $\mathscr{H}$. We see that this is not the case for the Wigner function, which is the same function for all members in any single equivalence class. For detection purposes, it is sufficient to use the overlap between two Wigner functions as given in Moyal's formula (5), because arccos and square root are monotone functions and do not alter the detection capabilities of a threshold detector.

5. EXPERIMENTAL RESULTS

5.1 Set up and data acquisition

The data employed for our analysis was kindly provided by the NQR group of King's College, London, under supervision of Professor J.A.S. Smith. A pure monoclinic TNT sample with a weight

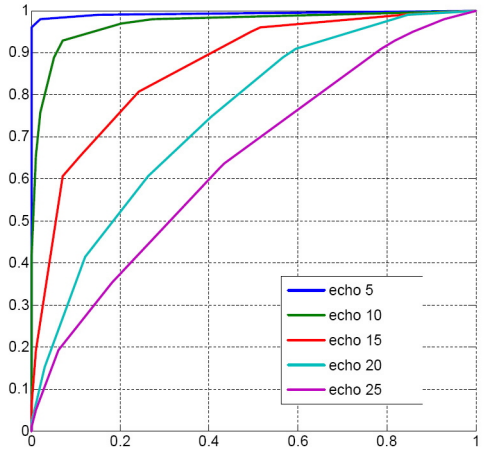

Figure 1: An improved demodulation detector using the three most distinct peaks in the NQR spectrum. Depicted are echoes 5, 10, 15, 20 and 25. The deterioration of the signal as a function of the echo number results in lower ROC curves.

typical of that found in an anti-personnel mine, is placed inside a solenoidal coil which emits an RF-pulse of the order of a kilo watt. The returned echo signal is routed through a hardware band-pass filter with a bandwidth of approximately 50 kHz and then sent to a Tecmag Libra spectrometer yielding a complex discrete time series. Because of the ideal laboratory conditions under which the signal has been obtained, the results will compare unrealistically optimistic with respect to those obtained under field conditions. In particular, the absence of RF interference and the use of a coil that contains the sample in its entirety, must be taken into account when attempting to compare the results of our analysis with those of data obtained under more realistic conditions. The emitted RF signals are pulsed, spin-locked echo signals with a mean excitation frequency of about 841.5 kHz. The mean and width of the excitation are such, that 4 spectral lines of TNT can be detected within the frequency range of the band pass filter. Because the same coil is used for the emission of the RF signal (which has a mean power of several kilo watts), as for the reception of the echo (which is extremely weak), the returned echo contains so-called antenna ringing effects, which are cancelled using a phase cycling technique well-known from NMR. The phase cycling technique requires forming an appropriate sum of four signals. The signals used for the analysis, are the sum of 5 such phase-cycled sums and hence consist of 20 repeated data acquisitions, averaged to improve signal to noise ratio. The sampling time is 5μs and each set has 8192 data points, which consists of 32 sequential echo signals, each containing 256 data points. The pulse sequence is of the type

$$\pi - \tau - \pi - 2\tau - \pi - 2\tau - \pi - 2\tau - \ldots$$

Here π denotes the RF pulses and the 1280 μs of data (256 times 5 μs) for each echo signal is acquired during the 2τ periods between the pulses. Algorithms are programmed in MATLAB 7 on a 2,2 GHz PC with 512 MB RAM and in all cases calculation time was less than one order of magnitude below the necessary data acquisition time. The calculation time necessary for the classification of a single echo requires 0.4 s for the Wigner-Ville method, whereas the improved demodulation technique requires 0.35 s.

5.2 The improved demodulation technique

The most simple and popular detection technique for NQR, is the so-called demodulation technique which first estimates the power

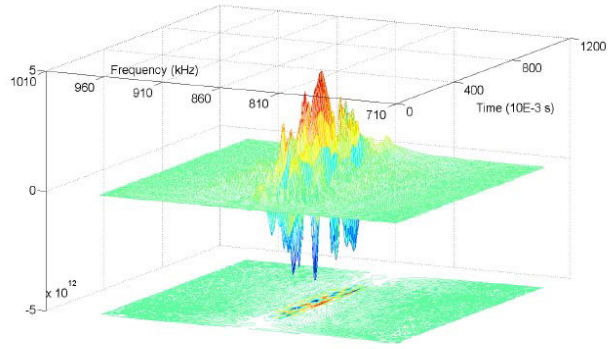

Figure 2: The Wigner-Ville function of the time series of the second spin echo. One can clearly see the signal is well-localized in the time-frequency plane. The maximum in time, as well as in frequency, is in the centre of the graph. Blue colors indicate negative values of the function.

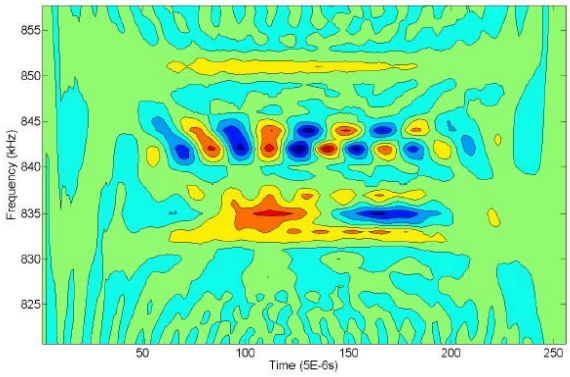

Figure 3: A projection of Figure 2 on the time-frequency plane yields a two-dimensional contour plot. As before, blue colors denote large negative values of the function, whereas orange-red colors indicates large positive values. We see the Wigner-Ville function has a strongly linear structure along single frequencies, oscillating along the time axis.

spectral density $S(\nu)$ of the signal $s(t_n)$, by taking the modulus squared of the fast (or discrete) Fourier transform of the discrete time series. If we call $\nu_{\max}$ the frequency $\nu_{\max} = \arg(\max(S(\nu)))$ where one expects the spectral line with the highest intensity in presence of TNT at a given temperature, the *estimated* power spectral density $\sigma(\nu_{\max})$ at this frequency $\nu_{\max}$, is the test statistic for a threshold detector. If $\sigma(\nu_{\max})$ exceeds a given threshold, the presence of TNT is accepted, if not, it is rejected. Sometimes the average under $\sigma(\nu_n)$ over a few frequency bins is taken as a statistical test parameter to account for drift in the transition frequencies as a result of the temperature dependence of the NQR spectrum. All our experimental samples are taken at the same temperature, hence we see no improvement in the efficiency of the method, whether we use $\sigma(\nu_{\max})$, or a sum of values $\sum\sigma(\nu_{\max})$ surrounding the relevant frequency bin. However, a considerable improvement is obtained when we allow for the demodulation technique to sample multiple peaks simultaneously. The results that we present here use this improved demodulation algorithm exploiting knowledge of the three dominant resonance frequencies of TNT within a range of a few tens of kHz around the mean excitation frequency 841.5 kHz. To calculate experimental ROC curves, we have taken 100 data samples with TNT, and 100 data samples without TNT. ROC curves are obtained by selecting a threshold value and calculating the sensitivity and specificity for that threshold and taking the convex hull of the resulting curve. The performance of the three peak demodulation technique can be inspected from the ROC curves depicted in 1. We see the first few echoes deliver a very reliable detector, but the statistical performance diminishes rapidly with increasing echo number.

5.3 The Time-Frequency method

To obtain a time-frequency perspective on this problem, we first calculate the Wigner-Ville distribution $W(t,\nu)$ of the complex discrete time series $s(t)$, averaged over a great number of experiments, which in our case was 99 time series. We will denote this Wigner function for the averaged signal by $\langle W(t,\nu)\rangle$. Note that no smoothing kernel or convolution of any kind has been applied. The result for the second spin echo can be seen in Figure 2. Due to the pulse scheme applied, the first spin echo is slightly different, but subsequent spin echoes deliver very similar, albeit less pronounced figures due to the poorer SNR.

Visual inspection of this graph shows the Wigner-Ville function is rather well-localized in the time-frequency plane. A projection of the function is shown at the bottom of Figure 2, but the distinct linear features can be better appreciated in a separate contour plot, as shown in Figure 3.To exploit the evident linear structure of the time-frequency quasi-distribution, we take three sections of the Wigner-Ville function at the location of the strongest oscillating frequencies, corresponding to the three frequencies used in the improved demodulation technique.

$$\phi_i(t) = W(t,\nu_i), i = 1,2,3$$

From Figure 3 we see that two of the ϕ functions oscillate more rapidly than the third ϕ. The frequency of oscillation of the interference terms in (3) is known [4] to depend on the time-frequency distance between the separate contributions. As can be inspected in Figure 3, the two fast oscillating modes are much closer to each other than the third one, explaining this behavior. To obtain a detector, we use the overlap between two Wigner functions (5), as this is a monotone function of the distance function (6) between the (three) ϕ_i obtained for a great number of measurements and the actually measured one in a single experiment. Our test statistic is then simply given by the discretized version of the overlap (5):

$$\lambda = \sum_{k=1}^{256} \phi_1(t_k)\langle\phi_1(t_k)\rangle + \phi_2(t_k)\langle\phi_2(t_k)\rangle + \phi_3(t_k)\langle\phi_3(t_k)\rangle$$

We have written $\langle\phi_1\rangle$ as an abbreviation for $\langle W(t,\nu_i)\rangle$, where it is understood that, for the purpose of testing data batch i , we have excluded the actually measured value ϕ_i from the batch of measurements used to calculate the average value $\langle\phi_i\rangle$ to avoid cross-contamination of the results. The results are given as ROC curves obtained by varying the threshold for the test statistic and are depicted in Figure 4. We see the method delivers an informative detector even for high echo numbers for which the SNR is about two orders of magnitude lower than necessary for a near perfect detector. For example, the time-frequency detector performs nearly as good for echo 25, as echo 15 for the improved demodulation detector.As the first echo already yields a perfect detector for both methods, there seems no obvious incentive to improve the detection capabilities. However, the spin-lattice relaxation constrains the time between the spin-locked pulses to a minimum of the order of 10 seconds. Hence the necessary data acquisition time for the each single data sample, is approximately 20 acquisitions*10 seconds = 200 seconds. In actual demining applications, the necessary acquisition time will further increase as a result of RF interference, other

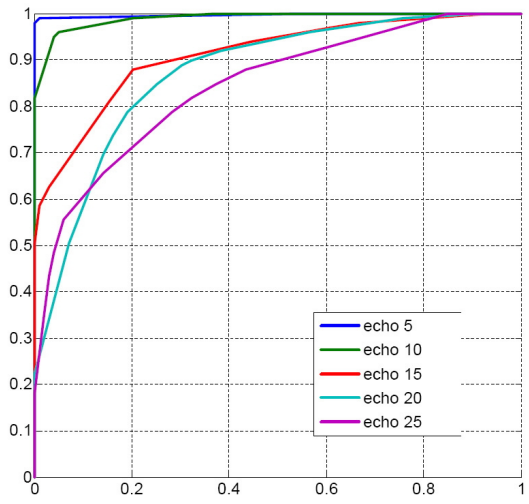

Figure 4: A time-frequency detector using three slices of the Wigner-Ville function at the three frequencies that correspond to the three frequencies used in the improved demodulation detector. Depicted are echoes 5, 10, 15, 20 and 25. Again we see the deterioration of the signal as a function of the echo number resulting in lower ROC curves. One can clearly see the time-frequency detector yields considerably better ROC curves than the demodulation technique, especially for higher echo numbers.

NQR active soil constituents such as piezoelectric ceramics, and the fact that only single sided (as opposed to the sample being *within* the coil, as is the case for our data), remote acquisition is possible. However, one can substantially decrease this acquisition time by combining the information in the different echoes. It is hence of vital importance to improve the detector performance for *all* the echoes in the pulse sequence.

6. CONCLUDING REMARKS

We have taken a time-frequency perspective on the analysis of data from NQR experiments in our search for increased sensitivity, or better still, a shorter acquisition time for NQR detectors used to remotely establish the presence of TNT. To evaluate the results a comparison was made with the popular demodulation detector. Because our method uses three slices of the Wigner-Ville quasi-distribution, we improved the demodulation technique accordingly by incorporating the intensities of the three dominant peaks in the experimentally obtained spectrum, leading to a substantially better ROC curves with respect to single frequency demodulation. Both the improved demodulation technique and the time-frequency approach are very fast and easy to implement. Our results indicate that even the improved demodulation technique yields substantially lower ROC curves than the proposed time-frequency analysis. Especially for signals of poor SNR, we see the demodulation technique performs comparable to the time-frequency approach used on signals with an SNR that is about a factor five lower. Handling signals with a low SNR is important, as one expects a deterioration of the already poor SNR inherent in NQR measurements in real-life demining applications.

7. ACKNOWLEDGEMENTS

This work was done as part of Flemish Fund for Scientific Research (FWO) research project G.0362.03N. We gratefully acknowledge J.A.S. Smith and M. Rowe for supplying us their NQR data and helpful feedback on our results. We thank Hichem Sahli, Luc van Kempen, Andreas Jakobsson and Sam Somasundaram for discussions and feedback.

REFERENCES

[1] T.P. Das and E.L. Hahn. Nuclear quadrupole resonance spectroscopy. Solid state physics. New York, Academic. Suppl. 1, 1958.

[2] Garroway A.N., Buess M. L., Miller J. B., Suits B. H., Hibbs A. D., Barrall G. A. , Matthews R. and Burnett L. J. , "Remote Sensing by Nuclear Quadrupole Resonance", IEEE Trans. Geoscience and Remote Sensing, vol. 39, no. 6, pp. 1108–1118, 2001.

[3] Y.K. Lee. Spin-1 "Nuclear quadrupole resonance theory with comparison to nuclear magnetic resonance." Concepts in Magnetic Resonance **14**, 3, 2002.

[4] P. Flandrin, Time-Frequency/Time-Scale Analysis, Academic Press, San Diego, 1999.

[5] V.T. Mikhalsevitch, T.N. Rudakov. "On the NQR detection of nitrogenated substances by multi-pulse sequences." Phys. stat. sol. (b), **241**, 2, pp 411-419, 2004.

[6] J.E. Moyal, Proc. Camb. Phil. Soc. vol. 45, 99 - 124, 1949

[7] F.E. Schroeck, Quantum Mechanics on Phase space. Kluwer Academic Publishers, Dordrecht, 1996.